



1 **Deciphering the Chemical Forms of Gaseous Oxidized**
2 **Mercury in Florida, USA**

3 Jiaoyan Huang¹, Matthieu B. Miller², Eric Edgerton³, Mae Sexauer Gustin²

4 ¹ Institute for the Environment, University of North Carolina, Chapel Hill, 100 Europa
5 Drive, Suite 490, Chapel Hill, NC, 27517, United States

6 ² Department of Natural Resources and Environmental Sciences, University of Nevada-
7 Reno, 1664 N. Virginia Street, Reno, NV, 89557, United States

8 ³ Atmospheric Research & Analysis, Inc., 410 Midenhall Way, Cary, North Carolina
9 27513, United States

10

11



12 **Abstract**

13 The highest mercury (Hg) wet deposition in the United States of America (USA) occurs
14 along the Gulf of Mexico, and in the southern and central Mississippi River Valley.
15 Gaseous oxidized Hg (GOM) is thought to be a major contributor due to high water
16 solubility and reactivity. Therefore, it is critical to understand concentrations, potential
17 for wet and dry deposition, and GOM compounds present in the air. Concentrations and
18 dry deposition fluxes of GOM were measured and calculated for Outlying Landing Field
19 (OLF), Florida, using data collected by a Tekran® 2537/1130/1135, the University of
20 Nevada-Reno Reactive Mercury Active System (UNRRMAS) with cation exchange and
21 nylon membranes, and Aerohead samplers that use cation-exchange membranes to
22 determine dry deposition. Relationships with Tekran® derived data must be interpreted
23 with caution, since GOM concentrations measured are biased low depending on the
24 chemical compounds in air, and interferences with water vapor and ozone. Criteria air
25 pollutants were concurrently measured.

26 Results from nylon membranes with thermal desorption analyses indicated five GOM
27 compounds in this area, including HgBr₂, HgO, Hg-nitrogen and sulfur compounds, and
28 an unknown compound. This indicates that the site is influenced by different gaseous
29 phase reactions and sources. Using back trajectory analysis a high GOM event related to
30 high CO, but average SO₂, indicated air parcels moved from the free troposphere, and
31 across Arkansas, Mississippi, and Alabama at low elevation (<300 m). This event was
32 initially characterized by HgBr₂ followed by a mixture of GOM compounds. GOM
33 chemistry indicates reactions with local mobile source pollutants and long range transport
34 from outside of the USA.

35 In order to develop methods to measure GOM concentrations and chemistry, and model
36 dry deposition processes, the actual GOM compounds need to be known, as well as their
37 corresponding physicochemical properties, such as Henry's Law constants.

38 *Keywords: multiple-resistance model, dry deposition, cation exchange membrane,*
39 *criteria pollutants, active samplers*

40



41 **1 Introduction**

42 Mercury (Hg) has been classified as a persistent, bioaccumulative toxin (PBT) (UNEP,
43 2013), and deposition from the atmosphere is considered the dominant pathway by which
44 Hg enters remote ecosystems (Lindberg et al., 2007). In some areas, scavenging by
45 precipitation controls atmospheric Hg removal processes, such as in the Southeastern
46 United States of America (USA), where precipitation amounts are high (Prestbo and Gay,
47 2009). However, wet deposition concentrations are not necessarily correlated with
48 precipitation amounts >81mm, and deposition did not decreased with emission reductions
49 as coal combustion facilities in the region have implemented control technologies
50 (Prestbo and Gay, 2009). A contributing factor to wet deposition in the Gulf Coast area
51 may be related to high atmospheric convection during thunderstorms and scavenging of
52 gaseous oxidized Hg (GOM) from the free troposphere (Nair et al., 2013), and down
53 mixing of air with high GOM from the free troposphere (cf. Gustin et al., 2012).

54 An additional concern is that the Tekran® system measurement currently used to
55 quantify GOM does not equally quantify all GOM forms, and has interferences with
56 water vapor and ozone (cf. Ambrose et al., 2013; Gustin et al., 2013; Huang et al., 2013;
57 Lyman et al., 2010; McClure et al., 2014; Lyman et al., 2016). Since GOM is considered
58 an important form that can be rapidly removed from the atmosphere due to high water
59 solubility (Lindberg et al., 2007); it is important to understand both atmospheric
60 concentrations and chemistry (i.e. specific chemical compounds). Use of the University
61 of Nevada-Reno Reactive Mercury Active System (UNRRMAS) that collects GOM on
62 nylon membranes in tandem with cation exchange membranes has indicated that there are
63 different chemical compounds in the air and concentrations are 2 to 13 time higher than
64 previously thought (Huang et al., 2013; Gustin et al., 2016).

65 Mercury has been studied in Florida for many years, initially because of the high
66 concentrations measured in fish and the Florida Panther (Dvonch et al., 1999; Gustin et
67 al., 2012; Marsik et al., 2007; Pancras et al., 2011; Peterson et al., 2012). Long-term
68 GEM and GOM concentrations as measured by the Tekran® system have declined;
69 however, PBM concentrations increased after 2009 (Edgerton, unpublished data),
70 suggesting the atmospheric chemistry has changed. Peterson et al. (2011) and Gustin et al.



71 (2012) suggested based on detailed assessment of passive sampler and Tekran® system
72 collected Hg data, criteria air pollutants, and meteorology that at 3 locations in Florida
73 different GOM compounds were present and these were generated by *in situ* oxidation
74 associated with pollutants generated by mobile sources, indirect and direct inputs of Hg
75 from local electricity generating plants, and direct input of Hg associated with long range
76 transport. At OLF, background deposition was equal to that associated with mobile
77 sources, and a significant component was derived from long range transport in the spring.

78 In this work, GOM collected using the UNRRMAS, and the Aerohead dry deposition
79 measurement method (Lyman et al., 2007; 2009) were analyzed, along with Tekran® Hg
80 and criteria air pollutant data to understand GOM chemistry and dry deposition at
81 Outlying Landing Field (OLF), located ~ 15 kilometers NW of Pensacola, Florida.
82 Mercury was measured concurrently with various trace gases (CO, O₃, SO₂, NO_x, NO_y)
83 and meteorology. Air GEM/GOM/PBM concentrations were measured by the Tekran®
84 2537/1130/1135 system, respectively.

85 GOM dry deposition fluxes were calculated using deposition velocities determined using
86 a multi-resistance model with ambient air GOM concentrations from the Tekran®
87 system (multiplied by a factor of 3 due to bias in the Tekran® system; cf. Huang and
88 Gustin, 2015), and compared to those obtained using Aerohead data. Results were used to
89 estimate dry deposition velocities for the GOM compounds observed. The hypothesis for
90 this work was that since GOM compounds can vary spatially and temporally, due to
91 different compounds produced by different sources and processes, this will result in
92 different dry deposition velocities and dry deposition flux.

93 **2 Methods**

94 2.1 Field site

95 The sampling site was located at OLF (30.550°N, 87.374°W, 44 m above sea level). The
96 closest major Hg emission source is a coal-fired power plant (Plant Crist) northeast of the
97 site (Figure 1). This area has been used for atmospheric Hg research in previous studies
98 (Caffrey et al., 2010; Lyman et al., 2009; Gustin et al., 2012; Peterson et al., 2012; Weiss-



99 Penzias et al., 2011). OLF is a coastal site (~25 km away from Gulf of Mexico)
100 influenced by sea breezes especially during the summer (Gustin et al., 2012). Based on
101 cluster analyses of data from one year at this location ~24% of the air comes from the
102 marine boundary layer during the day and 60% during the night (Figure 1).

103 2.2 Sampling Methods

104 Aerohead samplers for determination of dry deposition were deployed bi-weekly from
105 June 2012 to March 2014. UNRRAMS were deployed bi-weekly from March 2013 to
106 March 2014. Atmospheric Hg concentrations, including GEM, GOM, and PBM, were
107 measured using a Tekran® system (model 2357/1130/1135, Tekran® Instrument Corp.,
108 Ontario, Canada) that was operated with one-hour sampling and one-hour desorption with
109 detection limits of 0.1 ng m^{-3} , 1.5 pg m^{-3} , and 1.5 pg m^{-3} , respectively.

110 Reactive Hg (GOM + PBM) concentrations were measured using the UNRRAMS with 3
111 sets of two in-series 47 mm cation-exchange membranes (ICE450, Pall Corp., MI, USA).
112 Three sets of nylon membranes ($0.2 \mu\text{m}$, Cole-Parmer, IL, USA) were also deployed to
113 assess Hg compounds in the air. Cation exchange membranes have been demonstrated to
114 quantitatively measure specific compounds of GOM in the laboratory; however, may not
115 measure all compounds (Gustin et al., 2015; Gustin et al., 2016). Nylon membranes do
116 not retain GOM compounds quantitatively, and retention during transport needs to be
117 tested (Huang et al., 2013; Gustin et al., 2015; Gustin et al., 2016). Nylon membrane
118 retention is impacted by relative humidity that might limit uptake of specific forms.
119 Criteria air pollutants and meteorological data, including CO, SO₂, O₃, PM_{2.5}, NO, NO₂,
120 NO_y, temperature, relative humidity, wind speed, wind direction, pressure, solar radiation,
121 and precipitation were available at this site for the sampling period. See Peterson et al.
122 (2012) for detailed information on collection of these measurements.

123 Aeroheads and membranes were prepared at UNR, packed in a thermal isolated cooler,
124 and shipped back and forth between the laboratory and site. Samples were stored in a
125 freezer (-22°C) at UNR until analyzed. Cation-exchange membranes were digested and
126 analyzed following EPA Method 1631 E (Peterson et al., 2012), and nylon membranes
127 were first thermally desorbed, and then analyzed using EPA Method 1631 E (Huang et al.,



128 2013). Cation-exchange membrane blanks for Aerohead and UNRRAMS were 0.40 ± 0.18
129 ($n=42$), 0.37 ± 0.26 ($n=77$) ng, respectively; and for nylon membranes used in the active
130 system blanks were 0.03 ± 0.03 ($n=69$) ng. Therefore, method detection limits (MDL, 3-
131 sigma) for two-week sampling time (336 hrs) was $0.13 \text{ ng m}^{-2} \text{ hr}^{-1}$ for dry deposition,
132 respectively. For the active membrane system, the Hg amount on the back-up filters and
133 blanks were not significantly different (cation-exchange membrane: 0.4 ± 0.3 vs 0.4 ± 0.3
134 ng; nylon membrane: 0.03 ± 0.03 vs 0.02 ± 0.02 ng); therefore, the back-up filters were
135 included in the calculation of the bi-weekly blanks. The bi-weekly MDL (336 hrs) for
136 active system with cation-exchange and nylon membranes were 2-68 pg m^{-3} (mean: 24 pg
137 m^{-3}) and 0.01-14.6 pg m^{-3} (mean: 2.1 pg m^{-3}), respectively. Bi-weekly MDL was
138 calculated from 3 times the standard deviation of bi-weekly blanks. The MDL was
139 calculated for each period of sampling, due to the fact this can vary based on treatment of
140 the membranes, when preparing samples for deployment, deployment at the field site,
141 and handling once returned to the laboratory. The membranes may also vary by material
142 lot. All samples were corrected by subtracting the blank for the corresponding two-week
143 period.

144 2.3 Data analyses

145 Hourly Tekran®, criteria air pollutants, and meteorological data were managed and
146 validated by Atmospheric Research & Analysis, Inc (see Peterson et al., 2012). These
147 were then averaged into two-week intervals to merge with the membrane measurements.

148 In previous studies, scaling factors similar to HNO_3 ($\alpha=\beta=10$) were used to calculate
149 oxidized Hg dry deposition velocity (Marsik et al., 2007; Castro et al., 2012); however,
150 Lyman et al. (2007) used the effective Henry's Law constant, and half-redox reactions in
151 neutral solutions of HgCl_2 , and indicated HONO might better represent the chemical
152 properties of oxidized Hg rather than HNO_3 . Huang et al. (2015a) indicated that due to
153 limited understanding of oxidized Hg chemical properties, no single value can be used to
154 calculate oxidized Hg dry deposition, because α and β would change with different GOM
155 compounds. Here dry deposition was calculated using the multiple resistance model of
156 Lyman et al. (2007) using both $\alpha=\beta=2, 5, 7$, and 10.



157 Back trajectories were calculated using the Hybrid Single Particle Lagrangian Integrated
158 Trajectory (HYSPLIT 4.9) with EDAS 40-km, 1000-meter starting height. For day and
159 nighttime analyses, starting times were Local Standard Time (LST) 1100-1300 h and
160 100-300 h, 24-hour simulations. For a high-concentration event analyses, trajectories
161 were started for each day at 0000, 0400, 0800, 1200, 1600, and 2000 LST. Overall, the
162 uncertainties of back trajectories calculated from HYSPLIT are 20% of the air parcel
163 traveling distance (Draxler, 2013 ; Gebhart et al., 2005; Stohl, 1998; Stohl et al., 2003).
164 Back trajectories for the entire sampling time were analyzed using cluster analysis (Liu et
165 al., 2010).

166 Sigmaplot 14.0 (Systat Software Inc, San Jose, CA, USA), and Minitab 16.0 (Minitab
167 Inc., PA, US) were used to do t-tests and correlation analyses. Comparisons were
168 considered significantly different and correlations considered significant when $p < 0.05$.

169 **3 Results and Discussion**

170 3.1 Overall measurements

171 Similar to previous work at this location (Gustin et al., 2012), O₃ was highest in the
172 spring, and CO concentrations were high in winter due to a low boundary layer and
173 biomass burning, and low in summer (Table 1). Observations from the 3 GOM sampling
174 methods (Tekran®, and nylon, and cation exchange membranes) showed higher GOM
175 concentrations in spring relative to other seasons (Table 1). Concentrations of GOM
176 measured by cation-exchange membranes in the active system were significantly (p-value
177 < 0.05 , paired-t test) higher than those measured by Tekran® KCl-coated denuder and
178 nylon membranes, both of which have been reported to be influenced by relative
179 humidity (Huang and Gustin, 2015b; Gustin et al., 2015). Mean cation-exchange
180 membrane concentrations were higher than Tekran® derived GOM by 14, 48, 11, and 13
181 times in the spring, summer, fall and winter, respectively.

182 Nylon membranes collected higher GOM concentrations than those measured by the
183 Tekran® in spring 2013 when the humidity was low. Overall, air concentrations
184 measured by the Tekran® system in this study were similar to those measured in 2010



185 (Peterson et al., 2012). Particulate-bound Hg had the same diel trend as GOM, but higher
186 concentrations.

187 Understanding the oxidants present in air is important for understanding potential GOM
188 compounds. Oxidants to consider include O₃, halogenated compounds, sulfur and
189 nitrogen compounds (cf. Gustin et al., 2016). Since the active system is currently limited
190 to 2-week sampling period it is difficult to use the data collected to determine specific
191 sources; however, they are useful for understanding the specific compounds that might be
192 present, and this in turn can be used to understand sources.

193 3.2 Potential GOM compounds

194 Standard desorption profiles for GOM compounds obtained by Huang et al. (2013) and
195 Gustin et al. (2015) are compared to those obtained at OLF (Figure 2). Compounds in the
196 permeation tubes included HgBr₂, HgCl₂, HgN₂O₆•H₂O, HgSO₄, and HgO. HgCl₂ and
197 HgBr₂ have been identified as being released from permeation tubes (Lyman et al., 2016);
198 however, the exact N and S compounds are not known. Only during 10 periods the nylon
199 membranes (collected in triplicate) collected a significant amount of GOM based on their
200 bi-weekly detection limit (Figure 2), and their desorption profiles varied. Although data
201 are limited, because we have observed similar thermal desorption compounds in other
202 studies (i.e. Huang et al, 2013 and Gustin et al. 2016), this indicates different chemical
203 forms are being collected, and that the compounds are not being generated on the
204 membranes. This has been shown to be the case in a limited study (Pierce and Gustin,
205 2016). In addition to our work, two forms of GOM in Montreal Canada air were reported
206 (Deeds et al., 2015).

207
208 Five distinct patterns of release were observed during thermal desorption. One had a
209 high residual tail that does not match our standard profiles; however, was also observed
210 in Nevada (Gustin et al, 2016). These occurred on 4/2/2013, 4/9/2013 and 5/21/2013.
211 This suggests that in spring there is a compound that is unknown based on current
212 standard profiles. A nitrogen-based compound was found on 5/21/2013 based on the
213 desorption profile. The second pattern occurred on 3/19/2013 and 11/19/2013, and this



214 corresponds to HgBr_2 with some residual tail that is again some compound not accounted
215 for.

216

217 The third pattern that occurred on 5/7/2013 and 8/27/2013, and corresponds to Hg-
218 nitrogen based compound with a residual tail. The 4th pattern occurred on 1/14/2014, and
219 9/24/2013 was associated with HgSO_4 and the error bars are small. Lastly, the data
220 collected on 10/22/23 was noisy and had subtle peaks that correspond with HgO , a
221 nitrogen-based compound, and a high residual tail. It is interesting to note that the 11/19
222 profile was similar to HgCl_2 .

223 Previous studies reported consistent desorption profiles from 3 sites in Nevada and
224 California without significant point sources (Huang et al., 2013). Huang et al. (2013)
225 presented desorption profiles from a highway, agriculture, and marine boundary layer site.
226 Profiles from the marine boundary layer and agriculture impacted site did not show clear
227 residual tails at 185°C, but these were observed at the highway impacted site. In addition,
228 at OLF, a significant amount of GOM (15-30%) was released after 160 °C. This implies
229 that we are missing one or more GOM compound(s) (Figure 2) in our permeation profiles.
230 Interestingly, a peak was found in the 4/9/2013 sample at the GEM release temperature,
231 and this is not due to GEM absorption as demonstrated by Huang et al.(2013), and was
232 also observed in Nevada (Gustin et al., 2016), suggesting an additional unidentified
233 compound. This information indicates GOM compounds at OLF varied with time, and
234 this variation is due to complicated Hg emission sources and chemistry at this location (cf.
235 Gustin et al., 2012).

236 At OLF, GOM composition on the nylon membrane was more complicated than that
237 collected at rural sites in the Western US (cf. Huang et al.,2013; Gustin et al., 2016);
238 however, similar complexity was observed at a highway location in Reno, Nevada
239 (Gustin et al., 2016). Desorption curves from the nylon filters collected at rural locations
240 in Nevada were in the range of the standard GOM compounds that have been investigated
241 (Huang et al., 2013; Gustin et al., 2016). Curves with multiple peaks in this study imply
242 that there were at least 5 GOM compounds collected on the nylon membranes.



243 3.3 Dry deposition measurements

244 Dry deposition of GOM measured by the Aerohead sampler ranged from 0 to 0.5 ng m⁻²
245 hr⁻¹, and 83% of GOM dry deposition was higher than the detection limit (0.12 ng m⁻² hr⁻¹).
246 Higher GOM dry deposition was observed in spring relative to winter (ANOVA one-
247 way rank, p-value < 0.01); GOM dry deposition was slightly lower in summer and fall
248 (not statistically different) relative to the spring due to high wet deposition and
249 scavenging processes during these seasons. The pattern in GOM seasonal dry deposition
250 was similar to that reported by Peterson et al. (2012). However, GOM dry deposition
251 rates were significantly higher in this study than 2010 values (0.2 vs 0.05 ng m⁻² h⁻¹).
252 This is due to the correction of 0.2 ng m⁻² h⁻¹ applied in Peterson et al. (2012) to account
253 for contamination of the Aerohead that has been demonstrated to be unnecessary (Huang
254 et al., 2014). Although, highest GOM dry deposition measured using the Aerohead
255 sampler and GOM concentrations measured using the UNRRAMS were observed in
256 spring 2013, the value in March 2014 was relatively low. In March 2014, atmospheric
257 conditions were more similar to winter than spring, with low temperatures and high CO
258 concentrations. These results are different from those calculated using Tekran®
259 measurements that suggest low GOM concentrations and high deposition velocities, and
260 this is because the denuder measurements are biased low.

261 Modeled GOM dry deposition fluxes were calculated using GOM concentrations
262 measured by the Tekran® system that were multiplied by a factor of three (cf. Huang et
263 al., 2014). In general, measured Hg dry deposition fluxes were similar to those modeled
264 simulations with modeled GOM dry deposition $\alpha=\beta=2$ during winter, spring, and fall (see
265 below; Figure 3). However, measured Hg dry deposition was significantly higher than
266 modeled results (both $\alpha=\beta=2$ and 10) in summer and early fall (Figure 3). This indicates
267 there are compounds of GOM in the summer that are poorly collected by the denuder,
268 and this also can help explain the higher wet deposition measured during this season
269 (Prestbo and Gay, 2009). Highest deposition was measured during the spring, when the
270 input from long range transport is greatest (Gustin et al., 2012). Figure 3 shows the
271 disparity that occurs by season, and comparing model and measured values. For example



272 in spring $\alpha=\beta=10$ significantly overestimates deposition, while in the summer and early
273 fall measured deposition is greater than modeled values.

274 Because of the low GOM concentrations and influence of humidity on the nylon
275 membrane measurements (Huang and Gustin, 2015b), GOM compounds were identified
276 only in one summertime sample as $\text{HgN}_2\text{O}_6\cdot\text{H}_2\text{O}$. During this time, measured GOM dry
277 deposition was ~ 6 times higher than both modeled results, and considering the Tekran®
278 correction factor of 3, membrane-based $\text{HgN}_2\text{O}_6\cdot\text{H}_2\text{O}$ dry deposition flux was ~ 18 times
279 higher than the Tekran®-model-based value. Gustin et al. (2015) indicated $\text{HgN}_2\text{O}_6\cdot\text{H}_2\text{O}$
280 collection efficiency on cation-exchange membrane in charcoal scrubbed air was ~ 12.6
281 times higher than on Tekran (KCl-coated denuder).

282 However, in May 2013, two samples were dominated by a profile similar the Hg
283 nitrogen-based compound with lower measured/modeled ratios (2.1-6.0 with Tekran®
284 correction factor). This might be due to ambient air GOM chemistry being dominated by
285 a compound with a different dry deposition velocity, less interference on the denuder
286 surface, or parameters in the dry deposition scheme. In May, GOM concentrations
287 measured by the Tekran® were higher than in summer due to lower wet deposition and
288 mean humidity (Table 1). Therefore, despite the fact that GOM collection efficiency
289 associated with the Tekran and nylon membranes are impacted by environmental
290 conditions, this demonstrates the presence of different compounds in the air. The dry
291 deposition scheme needs Henry's Law constants for determining the scaling factors for
292 specific resistances for different compounds (Lyman et al., 2007; Zhang et al., 2002).

293 Lin et al. (2006) stated that the dry deposition velocity of HgO is two times higher than
294 that for HgCl_2 , due to the different Henry's Law constant. The Henry's Law constants for
295 HgCl_2 , HgBr_2 , and HgO presented in previous literature (Schroeder and Munthe, 1998)
296 have high uncertainty, for how these calculations were done is not clear (S. Lyman, Utah
297 State University, personal communication, 2015), and the constants for $\text{HgN}_2\text{O}_6\cdot\text{H}_2\text{O}$ and
298 HgSO_4 are unknown. Some researchers considered that GOM is similar to HNO_3
299 ($\alpha=\beta=10$), and some treated GOM as HONO ($\alpha=\beta=2$) (Castro et al., 2012; Lyman et al.,
300 2007; Marsik et al., 2007); however, using the parameters of HNO_3 could overestimate



301 GOM dry deposition velocities due to the differences of effective Henry's law constants
302 (HgCl_2 : $\sim 10^6$ HNO_3 ; $\sim 10^{13}$ M atm^{-1}).

303 If the ratios (HgBr_2 : 1.6, HgCl_2 : 2.4, HgSO_4 : 2.3, HgO : 3.7, and $\text{HgN}_2\text{O}_6\cdot\text{H}_2\text{O}$: 12.6) of
304 GOM concentrations measured by the Tekran® versus cation-exchange membranes for
305 different GOM permeated compounds (Gustin et al., 2015; Huang et al., 2013) are used
306 to correct Tekran® GOM data in this study, modeled GOM dry deposition (Figure 3) are
307 not correlated with measurements. For example, on 3/9/2013 and 11/19/2013 (Figure 3),
308 GOM was dominated by HgBr_2 and HgCl_2 . Dry deposition of HgBr_2 from Aerohead
309 measurements and modeling were close to $\alpha=\beta=10$; however, modeled and measured
310 HgCl_2 dry deposition were matched as $\alpha=\beta=2$. Average deposition velocity for $\alpha=\beta=2$
311 was 0.78 cm s^{-1} , and for $\alpha=\beta=10$ is 1.59 cm s^{-1} , if we assume the model is right. There
312 were three samples that were identified as Hg-nitrogen based compounds using nylon
313 membranes; however, the ratios of measurement and modeling $\text{HgN}_2\text{O}_6\cdot\text{H}_2\text{O}$ dry
314 deposition were inconsistent over time. In spring, all modeled $\text{HgN}_2\text{O}_6\cdot\text{H}_2\text{O}$ dry
315 deposition values were much higher than measured values; however, in summer,
316 measured and modeled $\text{HgN}_2\text{O}_6\cdot\text{H}_2\text{O}$ dry deposition were similar as $\alpha=\beta=5$ (Table 2). If
317 you assume the dry deposition measurements made by the surrogate surfaces are accurate
318 then this demonstrates there are different forms that occur over time, and these will have
319 different deposition velocities as suggested by Peterson et al. (2012).

320 3.4 Elevated Pollution Event

321 In spring 2013, there was a time period when high concentrations of O_3 , CO, and all Hg
322 measured (Figure 4). Figure 5 shows that during this time air masses traveled west to east
323 across the continent. The air movement pattern is similar to that found in Gustin et al.
324 (2012) for OLF Class 2 events which had low SO_2 concentrations. During this 4-week
325 period, air parcels traveling to OLF were in the free troposphere and descended to the
326 surface (Figure 5). Although there are coal-fired power plants in the upwind area within a
327 500 km range (Figure 1), the low SO_2 concentrations, and elevated CO, O_3 , and GOM
328 values were not from fossil fuel combustion. Gustin et al. (2012) also indicated that free
329 troposphere air impacted OLF. The first few endpoints for these trajectories indicate air



330 parcels entered North America at > 1000 m agl; therefore, there was transport of some air
331 measured during this time from the free troposphere. Ozone concentrations were also
332 similar to those measured in Nevada in the free troposphere at this time (Gustin et al.,
333 2014). It is important to note that the back trajectories are only for 72 hours and the ones
334 that subsided to surface levels in the Midwest were traveling fast. We hypothesize this is
335 a common event in the spring that represents free troposphere transport. The chemical
336 composition of this event suggests potential input from Asia as previously suggested for
337 numerous locations in Florida in the spring by Gustin et al. (2012). During this time
338 HgBr₂ was an important compound initially and then the profile was a gradual increase
339 with a high residual tail. This would suggest initial subsidence of air from the
340 stratosphere/troposphere (cf. Lyman et al., 2012) followed by a mixture of polluted air as
341 observed in the Western United States (c.f. VanCuren and Gustin, 2015)

342 **4 Conclusions**

343 The chemical forms of GOM in the atmosphere at OLF varied by season as suggested by
344 Gustin et al. (2012). Five potential different GOM compounds were identified at OLF
345 using nylon membranes with thermal desorption analysis, including HgBr₂, HgCl₂, HgO,
346 Hg-nitrogen and sulfur compounds, and 2 unknown compounds. Given the long sampling
347 time detailed assessment of specific sources is difficult, but the presence of different
348 compounds indicate multiple sources and different GOM chemistry. Comparing modeled
349 and measured Hg dry deposition fluxes also demonstrate there are different forms in air
350 and this will affect dry deposition velocities. In order to improve our understanding of Hg
351 air-surface exchange, and measure GOM physiochemical properties of different GOM
352 compounds need to be understood.

353 **5 Acknowledgements**

354 The authors thank The Southern Company (project manager-John Jansen) for their
355 support, and Bud Beghtel for deploying and collecting our membranes and passive
356 samplers at OLF and managing this site in general. This work was also supported by
357 EPRI and a National Science Foundation Grant 1326074. We thank the following
358 students for coordinating shipment of membranes and passive samplers, analyses of the



359 membranes in the lab, and keeping the glassware clean (Keith Heidecorn, Douglas Yan,
360 Matt Peckham, Jennifer Arnold, Jen Schoener, and Addie Luippold).

361 **6 References cited**

- 362 Ambrose, J.L., Lyman, S.N., Huang, J., Gustin, M.S., Jaffe, D.A., 2013. Fast Time
363 Resolution Oxidized Mercury Measurements during the Reno Atmospheric
364 Mercury Intercomparison Experiment (RAMIX). *Environmental Science &*
365 *Technology* 47, 7285-7294.
- 366 Belis, C.A., Karagulian, F., Larsen, B.R., Hopke, P.K., 2013. Critical review and meta-
367 analysis of ambient particulate matter source apportionment using receptor
368 models in Europe. *Atmospheric Environment* 69, 94-108.
- 369 Brooks, S., Ren, X., Cohen, M., Luke, W., Kelley, P., Artz, R., Hynes, A., Landing, W.,
370 Martos, B., 2014. Airborne Vertical Profiling of Mercury Speciation near
371 Tullahoma, TN, USA. *Atmosphere* 5, 557-574.
- 372 Caffrey, J.M., Landing, W.M., Nolek, S.D., Gosnell, K.J., Bagui, S.S., Bagui, S.C., 2010.
373 Atmospheric deposition of mercury and major ions to the Pensacola (Florida)
374 watershed: spatial, seasonal, and inter annual variability. *Atmos. Chem. Phys.* 10,
375 5425-5434.
- 376 Castell-Balaguer, N., Tellez, L., Mantilla, E., 2012. Daily, seasonal and monthly
377 variations in ozone levels recorded at the Turia river basin in Valencia (Eastern
378 Spain). *Environmental Science and Pollution Research* 19, 3461-3480.
- 379 Castro, M.S., Moore, C., Sherwell, J., Brooks, S.B., 2012. Dry deposition of gaseous
380 oxidized mercury in Western Maryland. *Science of The Total Environment* 417-
381 418, 232-240.
- 382 Choi, H.-D., Huang, J., Mondal, S., Holsen, T.M., 2013. Variation in concentrations of
383 three mercury (Hg) forms at a rural and a suburban site in New York State. *Sci.*
384 *Total Environ.* 448, 96-106, 2013.
- 385 Converse, A.D., Riscassi, A.L., Scanlon, T.M. 2014. Seasonal contribution of dewfall to
386 mercury deposition determined using a micrometeorological technique and dew
387 chemistry. *Journal of Geophysical Research-Atmospheres* 119, 284-292.
- 388 Deeds, D.A., Ghoshdastidar A., Raofie, F., Guerette, E.A., Tessier, .A, Ariya P.A. 2015
389
- 390
- 391 Development of a Particle-Trap Preconcentration-Soft Ionization Mass
392 Spectrometric Technique for the Quantification of Mercury Halides in Air.
393 *Analytical Chemistry* 87, 5109-5116
- 394 Dickerson, R.R., Rhoads, K.P., Carsey, T.P., Oltmans, S.J., Burrows, J.P., Crutzen, P.J.,
395 1999. Ozone in the remote marine boundary layer: A possible role for halogens.
396 *Journal of Geophysical Research: Atmospheres* 104, 21385-21395.



- 397 Draxler, R., 2013. What are the levels of uncertainty associated with back trajectory
398 calculations in HYSPLIT. NOAA.
- 399 Dvonch, J.T., Graney, J.R., Keeler, G.J., Stevens, R.K., 1999. Use of Elemental Tracers
400 to Source Apportion Mercury in South Florida Precipitation. *Environmental*
401 *Science & Technology* 33, 4522-4527.
- 402 Engle, M.A., Tate, M.T., Krabbenhoft, D.P., Kolker, A., Olson, M.L., Edgerton, E.S.,
403 DeWild, J.F., McPherson, A.K., 2008. Characterization and cycling of
404 atmospheric mercury along the central US Gulf Coast. *Applied Geochemistry* 23,
405 419-437.
- 406
- 407 Gay, D.A., Schmeltz, D., Prestbo, E., Olson, M.L., Sharac, T., Tordon, R., 2013. The
408 Atmospheric Mercury Network: measurement and initial examination of an
409 ongoing atmospheric mercury record across North America. *Atmos. Chem. Phys.*
410 13, 11339-11349.
- 411 Gebhart, K.A., Schichtel, B.A., Barma, M.G., 2005. Directional biases in back
412 trajectories caused by model and input data. *J. Air Waste Manage. Assoc* 55,
413 1649-1662
- 414 Gustin, Mae Sexauer, Pierce, Ashley M., Huang, Jiaoyan, Miller, Matthieu B., Holmes,
415 Heather,
416 S., Loria-Salazar, S. Marcela (2016) Evidence for different reactive Hg sources
417 and chemical compounds at adjacent valley and high elevation locations,
418 *Environmental Science and Technology*, accepted.
- 419
- 420 Gustin, M., Amos, H.M., Huang, J., Jaffe, D., Miller, M., Heidecorn, K., submitted to
421 ACP. Successes and challenges of measuring and modeling atmospheric mercury
422 at the part per quadrillion level. *Atmos. Chem. Phys.*
- 423 Gustin, M., Weiss-Penzias, P., Peterson, C., 2012. Investigating sources of gaseous
424 oxidized mercury in dry deposition at three sites across Florida, USA.
425 *Atmospheric Chemistry & Physics* 12, 9201-9219.
- 426 Gustin, M.S., Huang, J., Miller, M.B., Peterson, C., Jaffe, D.A., Ambrose, J., Finley, B.D.,
427 Lyman, S.N., Call, K., Talbot, R., Feddersen, D., Mao, H., Lindberg, S.E., 2013.
428 Do We Understand What the Mercury Speciation Instruments Are Actually
429 Measuring? Results of RAMIX. *Environmental Science & Technology* 47, 7295-
430 7306.
- 431 Gustin, M. S. , Amos, H. A, Huang, J., Miller, M.B., Heidecorn. 2015 Successes and
432 challenges of measuring and modeling atmospheric mercury at the part per
433 quadrillion level, Invited paper- Special Issue of Atmospheric Chemistry and
434 Physics. *Atmospheric Physics and Chemistry Discussions*, 15: 3777-3821,2015
- 435 Gustin, M. S. , Amos, H. A, Huang, J., Miller, M.B., Heidecorn. 2015 Measuring and
436 modeling
437 mercury in the atmosphere: A critical review, Invited paper- Special Issue of
438 Atmospheric Chemistry and Physics. *Atmospheric Physics and Chemistry*, 15:
439 5697-2015. doi: 10.5194/acp-15-5697-2015.
- 440 Heidecorn et al., in progress for this Special Issue



- 441 Huang, J., Choi, H.-D., Hopke, P.K., Holsen, T.M., 2010. Ambient Mercury Sources in
442 Rochester, NY: Results from Principle Components Analysis (PCA) of Mercury
443 Monitoring Network Data. *Environmental Science & Technology* 44, 8441-8445.
- 444 Huang, J., Gustin, M., 2015a, Uncertainties of Gaseous Oxidized Mercury Measurements
445 Using KCl-coated Denuders, Cation-Exchange Membranes, and Nylon
446 Membranes: Humidity Influences, *Environmental Science and Technology*,
447 49, 432-441
- 448 Huang, J., Lyman, S.N., Hartman, J.S., Gustin, M.S., 2014. A review of passive sampling
449 systems for ambient air mercury measurements. *Environmental Science:
450 Processes & Impacts* 16, 374-392.
- 451 Huang, J., Miller, M.B., Weiss-Penzias, P., Gustin, M.S., 2013. Comparison of Gaseous
452 Oxidized Hg Measured by KCl-Coated Denuders, and Nylon and Cation
453 Exchange Membranes. *Environmental Science & Technology* 47, 7307-7316.
- 454 Huang, J., Gustin, M.S. 2015b Use of passive sampling methods and models to understand
455 sources of mercury deposition to high elevation sites in the Western United States.
456 *Environmental Science and Technology*, 49 (432-441) DOI 10.1021/es502836w
- 457 Jackson, J.E., 1991 *A User's Guide to Principal Components*. Wiley.
- 458 Johnson, J.E., Gammon, R.H., Larsen, J., Bates, T.S., Oltmans, S.J., Farmer, J.C., 1990.
459 Ozone in the marine boundary layer over the Pacific and Indian Oceans:
460 Latitudinal gradients and diurnal cycles. *Journal of Geophysical Research:
461 Atmospheres* 95, 11847-11856.
- 462 Landing, W.M., Caffrey, J.M., Nolek, S.D., Gosnell, K.J., Parker, W.C., 2010.
463 Atmospheric wet deposition of mercury and other trace elements in Pensacola,
464 Florida. *Atmos. Chem. Phys.* 10, 4867-4877.
- 465 Landis, M.S., Lewis, C.W., Stevens, R.K., Keeler, G.J., Dvonch, J.T., Tremblay, R.T.,
466 2007. Ft. McHenry tunnel study: Source profiles and mercury emissions from
467 diesel and gasoline powered vehicles. *Atmospheric Environment* 41, 8711-8724.
- 468 Landis, M.S., Stevens, R.K., Schaedlich, F., Prestbo, E.M., 2002. Development and
469 Characterization of an Annular Denuder Methodology for the Measurement of
470 Divalent Inorganic Reactive Gaseous Mercury in Ambient Air. *Environmental
471 Science & Technology* 36, 3000-3009.
- 472 Lin, C.-J., Pongprueksa, P., Lindberg, S.E., Pehkonen, S.O., Byun, D., Jang, C., 2006.
473 Scientific uncertainties in atmospheric mercury models I: Model science
474 evaluation. *Atmospheric Environment* 40, 2911-2928.
- 475 Lindberg, S.E., Bullock, R., Ebinghaus, R., Engstrom, D., Feng, X., Fitzgerald, W.,
476 Pirrone, N., Prestbo, E., Seigneur, C., 2007. A synthesis of progress and
477 uncertainties in attributing the sources of mercury in deposition. *AMBIO* 36, 19-
478 32.
- 479 Liu, B., Keeler, G.J., Timothy Dvonch, J., Barres, J.A., Lynam, M.M., Marsik, F.J.,
480 Morgan, J.T., 2010. Urban-rural differences in atmospheric mercury speciation.
481 *Atmospheric Environment* 44, 2013-2023.
- 482 Lyman, Seth; Jones, Colleen; O'Neil, Trevor; Allen, Tanner; Miller, Matthieu; Gustin,
483 Mae;
484 Pierce, Ashley; Luke, Winston; Ren, Xinrong; Kelley (2016) Automated
485 Calibration of Atmospheric Oxidized Mercury Measurements submitted to
486 *Environmental Science and Technology*



- 487
488 Lyman, S.N., Gustin, M.S., Prestbo, E.M., Marsik, F.J., 2007. Estimation of Dry
489 Deposition of Atmospheric Mercury in Nevada by Direct and Indirect Methods.
490 Environmental Science & Technology 41, 1970-1976.
- 491 Lyman S.N., Gustin, M.S., Prestbo, E.M., Kilner, P.I., Edgerton, E., Hartsell, B. 2009.
492 Testing and Application of Surrogate Surfaces for Understanding Potential
493 Gaseous Oxidized Mercury Dry Deposition. Environmental Science &
494 Technology 43, 6235-6241.
- 495
496 Lyman, S.N., Jaffe, D.A., 2012. Formation and fate of oxidized mercury in the upper
497 troposphere and lower stratosphere. Nat. Geosci. 5, 114-117.
- 498 Lyman, S.N., Jaffe, D.A., Gustin, M.S., 2010. Release of mercury halides from KCl
499 denuders in the presence of ozone. Atmospheric Chemistry & Physics 10, 8197-
500 8204.
- 501 Marsik, F.J., Keeler, G.J., Landis, M.S., 2007. The dry-deposition of speciated mercury
502 to the Florida Everglades: Measurements and modeling. Atmospheric
503 Environment 41, 136-149.
- 504 McClure, C.D., Jaffe, D.A., Edgerton, E.S., 2014. Evaluation of the KCl Denuder
505 Method for Gaseous Oxidized Mercury using HgBr₂ at an In-Service AMNet Site.
506 Environmental Science & Technology 48, 11437-11444.
- 507 Nair, U.S., Wu, Y., Holmes, C.D., Ter Schure, A., Kallos, G., Walters, J.T., 2013. Cloud-
508 resolving simulations of mercury scavenging and deposition in thunderstorms.
509 Atmos. Chem. Phys. 13, 10143-10157.
- 510 NOAA, 2008. Eta Data Assimilation System (EDAS40) Archive Information, Silver
511 Spring, MD.
- 512 Pancras, J.P., Vedantham, R., Landis, M.S., Norris, G.A., Ondov, J.M., 2011. Application
513 of EPA Unmix and Nonparametric Wind Regression on High Time Resolution
514 Trace Elements and Speciated Mercury in Tampa, Florida Aerosol.
515 Environmental Science & Technology 45, 3511-3518.
- 516 Peterson, C., Alishahi, M., Gustin, M.S., 2012. Testing the use of passive sampling
517 systems for
518 understanding air mercury concentrations and dry deposition across Florida, USA.
519 Science of The Total Environment 424, 297-307.
- 520 Pierce, A. M., Gustin, M. S. 2016 Development of a particulate mass measurement
521 system for
522 tracing pollution sources using atmospheric mercury concentrations submitted to
523 Environmental Science and Technology
524
- 525 Prestbo, E.M., Gay, D.A., 2009. Wet deposition of mercury in the U.S. and Canada,
526 1996-2005: Results and analysis of the NADP mercury deposition network
527 (MDN). Atmospheric Environment 43, 4223-4233.
- 528 Schroeder, W.H., Munthe, J., 1998. Atmospheric mercury--An overview. Atmospheric
529 Environment 32, 809-822.
- 530 Seinfeld, J.H., Pandis, S.N., 2006. Atmospheric Chemistry and Physics. John Wiley &
531 Sons, Inc., Hoboken, New Jersey.



- 532 Song, F., Shin, J.Y., Jusino-Atresino, R., Gao, Y., 2011. Relationships among the
533 springtime ground-level NO_x, O₃ and NO₃ in the vicinity of highways in the US
534 East Coast. *Atmos. Poll. Res.* 2, 374-383.
- 535 Stohl, A., 1998. Computation, accuracy and applications of trajectories - a review and
536 bibliography. *Atmospheric Environment* 32, 947-966.
- 537 Stohl, A., Forster, C., Eckhardt, S., Spichtinger, N., Huntrieser, H., Heland, J., Schlager,
538 H., Wilhelm, S., Arnold, F., Cooper, O., 2003. A backward modeling study of
539 intercontinental pollution transport using aircraft measurements. *J. Geophys. Res.*
540 108, 4370; DOI: 10.1029/2002JD002862
- 541 VanCuren R, Gustin MS. Identification of sources contributing to PM_{2.5} and ozone at
542 elevated sites in the western US by receptor analysis: Lassen Volcanic National
543 Park, California, and Great Basin National Park, Nevada. *Science of the Total*
544 *Environment* 2015; 530: 505-518.
- 545 UNEP, 2013. Global Mercury Assessment 2013-Sources, Emissions, Releases, and
546 Environmental Transport. UNEP Division of Technology, Industry and
547 Economics, Chemicals Branch International Environment House
- 548 Weiss-Penzias, P., Jaffe, D., Swartzendruber, P., Hafner, W., Chand, D., Prestbo, E.,
549 2007. Quantifying Asian and biomass burning sources of mercury using the
550 Hg/CO ratio in pollution plumes observed at the Mount Bachelor observatory.
551 *Atmospheric Environment* 41, 4366-4379.
- 552 Weiss-Penzias, P., Jaffe, D.A., McClintick, A., Prestbo, E.M., Landis, M.S., 2003.
553 Gaseous Elemental Mercury in the Marine Boundary Layer: Evidence for Rapid
554 Removal in Anthropogenic Pollution. *Environmental Science & Technology* 37,
555 3755-3763.
- 556 Weiss-Penzias, P.S., Gustin, M.S., Lyman, S.N., 2011. Sources of gaseous oxidized
557 mercury and mercury dry deposition at two southeastern U.S. sites. *Atmospheric*
558 *Environment* 45, 4569-4579.
- 559 Zhang, L., Brook, J.R., Vet, R., 2003. A revised parameterization for gaseous dry
560 deposition in air-quality models. *Atmos. Chem. Phys.* 3, 2067-2082.
- 561 Zhang, L., Moran, M.D., Makar, P.A., Brook, J.R., Gong, S., 2002. Modelling gaseous
562 dry deposition in AURAMS: a unified regional air-quality modelling system.
563 *Atmospheric Environment* 36, 537-560.
- 564
565
566



567 Table 1 – Overall seasonal average of air species, GEM, PBM, GOM (measured using
 568 three different methods) concentration, GOM dry deposition (DD), and meteorological
 569 data at OLF.

	2012			2013				2014
	Summer	Fall	Winter	Spring	Summer	Fall	Winter	March
Ozone [ppb]	30±15	30±12	29±11	38±12	24±12	26±11	27±10	35±12
CO [ppb]	143±38	161±35	167±41	165±36	139±35	156±33	167±35	183±33
SO ₂ [ppb]	0.3±0.4	0.6±1.5	0.4±0.5	0.3±0.5	0.2±0.3	0.4±0.5	0.7±1.2	0.3±0.4
NO [ppb]	0.3±0.7	0.3±0.7	0.3±0.8	0.2±0.5	0.3±0.7	0.3±0.8	0.4±0.8	0.2±0.5
NO ₂ [ppb]	2.4±2.4	3.0±2.7	3.0±3.1	2.0±2.3	2.2±2.1	3.1±2.9	3.2±3.0	2.3±2.8
NO _x [ppb]	3.6±2.9	4.3±3.1	4.3±3.6	3.1±2.8	3.2±2.5	4.4±3.3	4.2±3.4	3.6±3.1
GEM [ng m ⁻³] ^a	1.2±0.1	1.2±0.1	1.3±0.1	1.2±0.2	1.1±0.1	1.0±0.1	1.2±0.3	1.2±0.1
GOM [pg m ⁻³] ^a	0.6±1.3	1.1±2.8	1.0±2.2	2.9±5.1	0.5±1.0	1.1±2.1	1.3±2.5	2.0±3.6
PBM [pg m ⁻³] ^a	2.4±2.6	3.6±3.8	7.3±8.7	5.9±6.8	2.3±2.0	2.9±2.3	4.9±5.3	4.0±3.4
GOM [pg m ⁻³] ^b	-	-	-	43±110	24±57	14±18	17±23	24±15
GOM [pg m ⁻³] ^c	-	-	-	4±10	0.4±1.3	1.2±1.1	0.6±0.6	0.6±0.5
GOM DD [ng m ⁻² hr ⁻¹]	0.24±0.20	0.17±0.12	0.15±0.06	0.40±0.23	0.20±0.13	0.13±0.18	0.20±0.50	0.14±0.04
WS [m s ⁻¹]	2.1±1.2	2.1±1.0	2.8±1.7	2.9±1.8	2.0±1.1	2.1±1.1	2.5±1.3	2.5±1.5
TEMP [°C]	26±3	19±6	14±6	18±6	26±3	20±7	11±7	14±5
RH [%]	83±14	76±18	79±19	73±21	84±13	77±17	76±23	78±21
SR [w m ⁻²]	230±302	193±271	121±199	266±304	210±278	175±255	129±212	182±278
Precipitation [mm]	637	186	385	223	1010	254	357	183

570

571 ^a: Tekran data572 ^b: cation-exchange membrane data573 ^c: nylon membrane data

574



Table 2 – Modeled (multiple-resistance model) and measured (surrogate surfaces) GOM dry deposition ($\text{ng m}^{-2} \text{hr}^{-1}$), GOM concentrations used to calculate for modeled results are from the Tekran® data and corrected by compounds' corresponding ratios from Gustin et al. (submitted). The sample with unknown compound is used the Tekran® data with correction factor of three (average ratio). The tentative GOM compounds are identified from nylon membrane results.

Start date	Tentative GOM compound	Measured GOM dry deposition flux	Modeled GOM dry deposition $\alpha=\beta=2$	Modeled GOM dry deposition $\alpha=\beta=5$	Modeled GOM dry deposition $\alpha=\beta=7$	Modeled GOM dry deposition $\alpha=\beta=10$
3/12/2013	HgBr ₂	0.50±0.06	0.34	0.49	0.54	0.58
3/26/2013	unknown	0.40±0.11	0.34	0.47	0.52	0.56
4/30/2013	Hg(NO ₃) ₂	0.50±0.13	1.21	1.67	1.81	1.95
5/14/2013	Hg(NO ₃) ₂	0.40±0.09	1.19	1.69	1.88	2.07
8/20/2013	Hg(NO ₃) ₂	0.15±0.07	0.10	0.14	0.16	0.17
11/12/2013	HgCl ₂	0.08±0.03	0.11	0.16	0.17	0.19
1/7/2014	HgSO ₄	0.19±0.03	0.18	0.24	0.27	0.29



Figure Caption

Figure 1 – Sampling site and point sources (NEI 2011) map. Cluster trajectories for daytime (11:00-13:00) and nighttime (1:00-3:00).

Figure 2 – Desorption profiles from nylon membranes with standard materials in laboratory investigation (top) and field measurements. Whisker is 1 standard variation, and only present in the desorption peak. Note the Hg-nitrogen compound in the permeation tube was $\text{HgN}_2\text{O}_6 \cdot \text{H}_2\text{O}$.

Figure 3 – Measured and modeled GOM dry deposition fluxes, Tekran® data (correction factor of three) were used with multiple resistance models ($\alpha=\beta=2$ and 10). Tentative GOM compounds were determined using the results from nylon membranes desorption.

Figure 4 – Temporal variation of GOM concentrations (mean \pm standard deviation, bi-week average), outlined rectangle indicates a polluted event with high Hg, CO, and ozone concentrations. Data are missing for 3 weeks because it was not collected. Tekran data is presented when $>75\%$ of the data were available and membrane data are shown when above the method detection limit.

Figure 5 – Results of gridded frequency distribution (left), light color indicates less endpoints in a grid. Altitude of 72-hr trajectories during the polluted event (3/12/2013-4/2/2013), light color of dots on left panel represents low altitude.

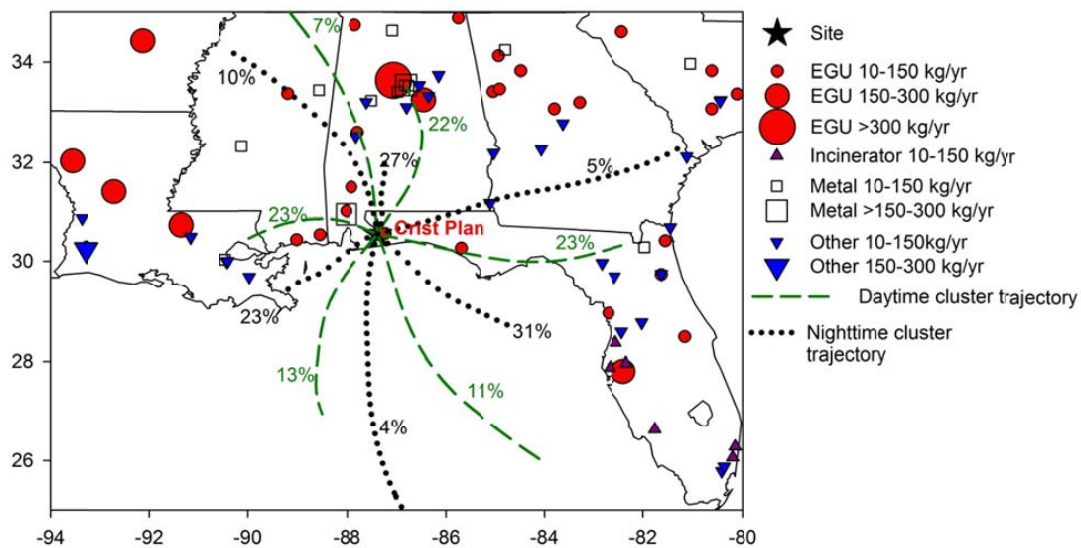


Figure 1 – Sampling site and point sources (NEI 2011) map. Cluster trajectories for daytime (11:00-13:00) and nighttime (1:00-3:00).

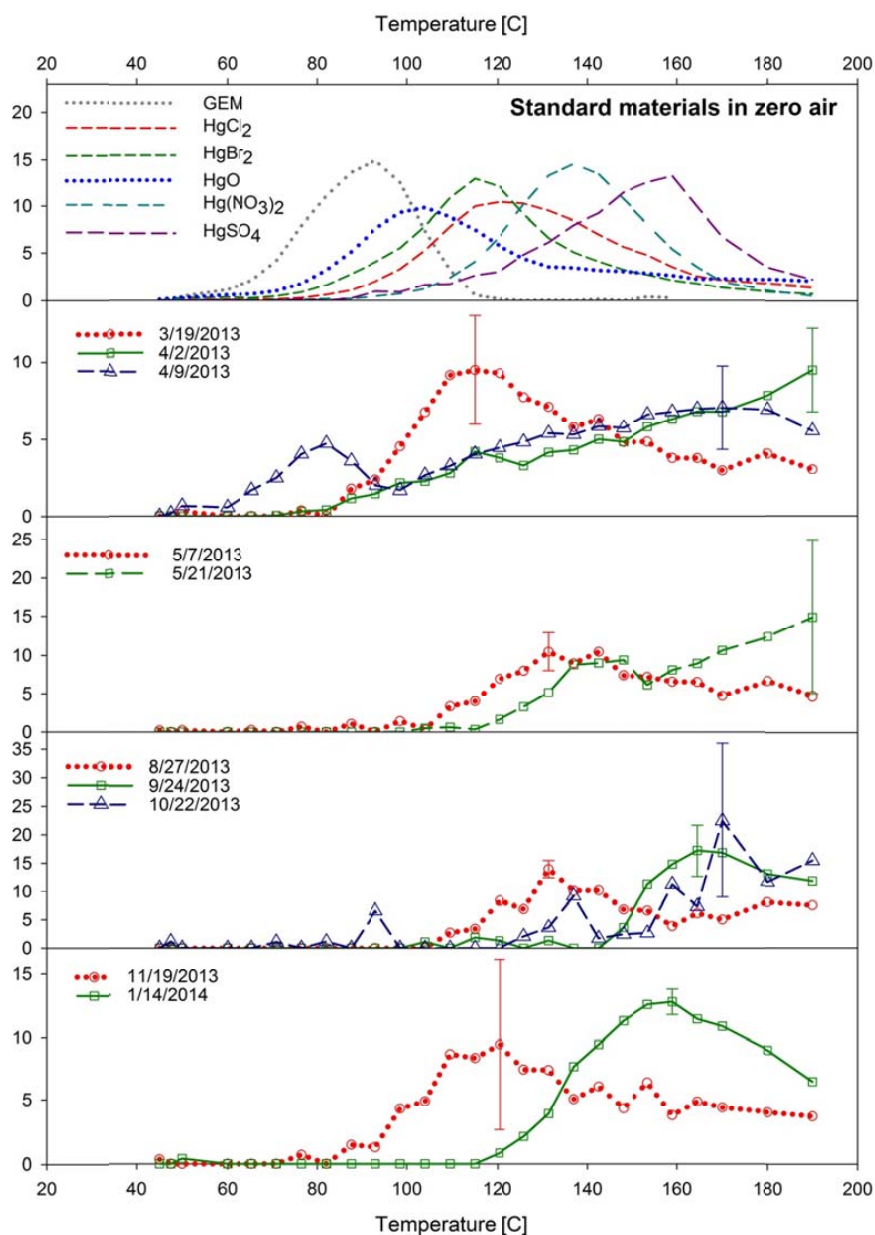


Figure 2 – Desorption profiles from nylon membranes with standard materials in laboratory investigation (top) and field measurements. Whisker is 1 standard variation, and only present in the desorption peak. Note the Hg-nitrogen compound in the permeation tube was $\text{HgN}_2\text{O}_6 \cdot \text{H}_2\text{O}$.

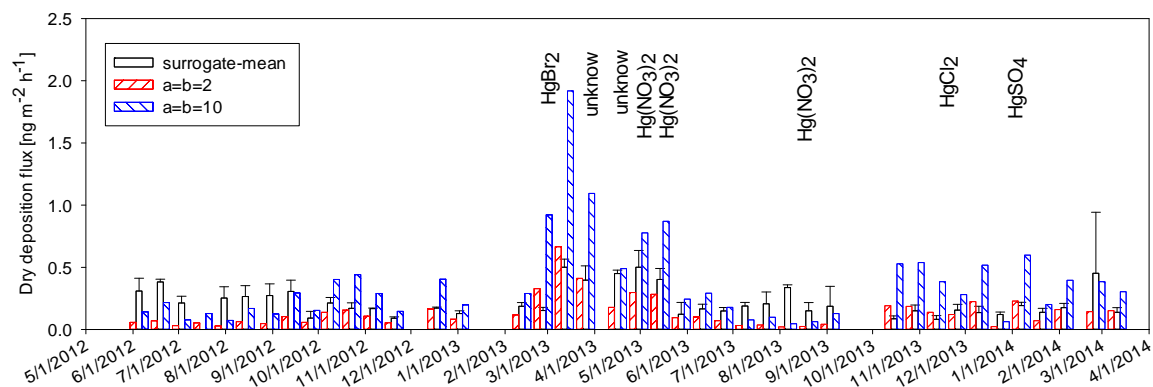
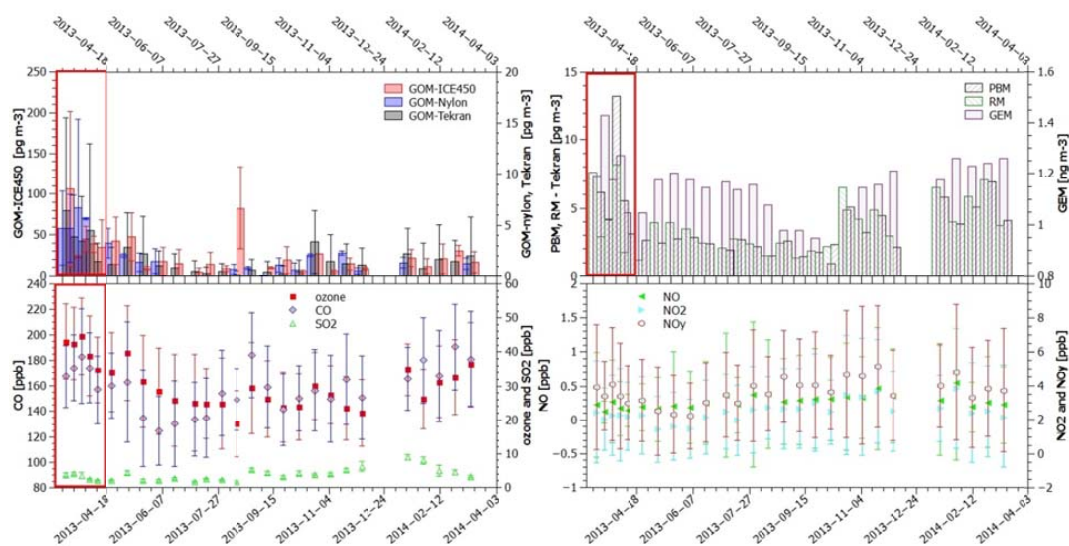


Figure 3 – Measured and modeled GOM dry deposition fluxes, Tekran® data (correction factor of three) were used with multiple resistance models ($\alpha=\beta=2$ and 10). Tentative GOM compounds were determined using the results from nylon membranes desorption.



1

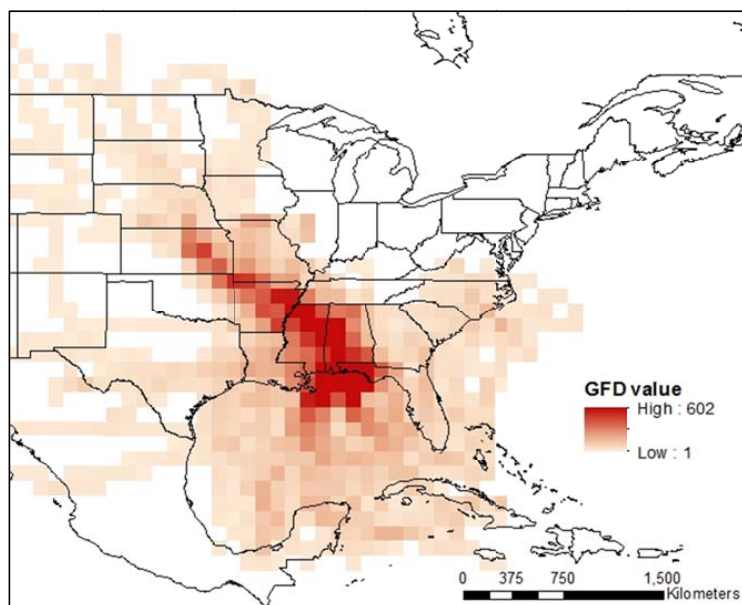


2

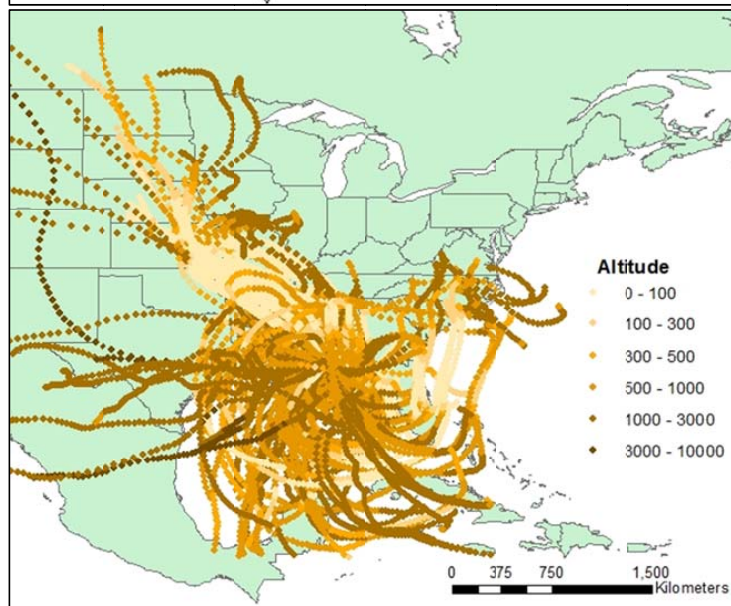
3 Figure 4 – Temporal variation of GOM concentrations (mean \pm standard deviation, bi-week
4 average), outlined rectangle indicates a polluted event with high Hg, CO, and ozone
5 concentrations. Data are missing for 3 weeks because it was not collected. Tekran data is
6 presented when $>75\%$ of the data were available and membrane data are shown above the
7 method detection limit.



8



9



10

11 Figure 5 – Results of gridded frequency distribution (left), light color indicates less endpoints in
12 a grid. Altitude of 72-hr trajectories during the polluted event (3/12/2013-4/2/2013), light color
13 of dots on left panel represents low altitude.
14